© 2020. Published by The Company of Biologists Ltd | Development (2020) 147, dev183798. doi:10.1242/dev.183798

TECHNIQUES AND RESOURCES

RESEARCH REPORT

# Germline development in rat revealed by visualization and deletion of *Prdm14*

**Toshihiro Kobayashi[1,2,*], Hisato Kobayashi[3,*], Teppei Goto[1,‡], Tomoya Takashima[4,‡], Mami Oikawa[1], Hiroki Ikeda[3], Reiko Terada[1], Fumika Yoshida[1], Makoto Sanbo[1], Hiromitsu Nakauchi[5,6], Kazuki Kurimoto[3] and Masumi Hirabayashi[1,2,§]**

## ABSTRACT

Primordial germ cells (PGCs), the founder cells of the germline, are specified in pre-gastrulating embryos in mammals, and subsequently migrate towards gonads to mature into functional gametes. Here, we investigated PGC development in rats, by genetically modifying *Prdm14*, a unique marker and an essential PGC transcriptional regulator. We trace PGC development in rats, for the first time, from specification until the sex determination stage in fetal gonads using *Prdm14 H2BVenus* knock-in rats. We uncover that the crucial role of *Prdm14* in PGC specification is conserved between rat and mice, by analyzing *Prdm14*-deficient rat embryos. Notably, loss of *Prdm14* completely abrogates the PGC program, as demonstrated by failure of the maintenance and/or activation of germ cell markers and pluripotency genes. Finally, we profile the transcriptome of the post-implantation epiblast and all PGC stages in rat to reveal enrichment of distinct gene sets at each transition point, thereby providing an accurate transcriptional timeline for rat PGC development. Thus, the novel genetically modified rats and data sets obtained in this study will advance our knowledge on conserved versus species-specific features for germline development in mammals.

**KEY WORDS: Prdm14, Primordial germ cell, Rat**

## INTRODUCTION

The germline is a unique cell lineage capable of transmitting genetic information to the next generation. In mammals, all germline cells, including sperm and eggs, originate from primordial germ cells (PGCs) specified from the pluripotent epiblast in pre-gastrulating embryos (Saitou and Yamaji, 2012; Tang et al., 2016). Studying PGC specification and development is important for understanding the fundamentals of cell fate determination as well as the mechanisms underlying disease and infertility.

Germline development in mammals has been extensively studied in the mouse model system. Loss-of-function studies using knockout mice has led to the identification of essential inductive signals for PGC fate: WNT and BMP (Aramaki et al., 2013; Lawson et al., 1999; Ohinata et al., 2009; Ying and Zhao, 2001), and the downstream core transcriptional regulators Prdm1 (also called Blimp1), Prdm14 and Tfap2c (also called Ap2γ) (Ohinata et al., 2005; Weber et al., 2010; Yamaji et al., 2008). Furthermore, remarkable progress in reconstituting germline development *in vitro* from mouse pluripotent stem cells (Hayashi et al., 2012, 2011; Hikabe et al., 2016) has enabled comprehensive analysis (Kurimoto et al., 2015; Shirane et al., 2016) and large-scale genetic screening (Hackett et al., 2018), which was difficult previously due to the limited number of nascent PGCs *in vivo*.

Here, we examine germline development in the rat model system. Rats are widely used as laboratory animals. Many genetic and physiological features of rats are much closer to humans than those of mice are (Aitman et al., 2008). The study of rats, as the closest laboratory animal to mice, is essential to determine conserved mechanisms of germline development among rodents. Nevertheless, only limited information on the rat germline is available, likely due to the lack of appropriate genetically modified lines. Histological analysis to identify rat PGCs by morphology (Beaumont and Mandl, 1963), alkaline phosphatase activity (Kemper and Peters, 1987) and immunostaining of some representative markers (Encinas et al., 2012; Leitch et al., 2010; Northrup et al., 2011) have provided a rough timeline for rat germline development. In a recent report, to visualize gonadal to adult germ cells *in vivo*, *Ddx4-EGFP* transgenic rats were generated (Gassei et al., 2017). However, owing to the absence of *Ddx4* expression in earlier PGCs, the specification and migration stages of rat PGCs have not yet been documented. Thus, by using novel genetically modified rats, we aimed to collect fundamental information, such as developmental timing and gene expression changes during germline development in rats, to compare with the well-studied mouse model.

Of the unique and important regulators for mammalian germline, we focused on *Prdm14*, a PR domain-containing transcriptional regulator. In mice, *Prdm14* is specifically expressed in pluripotent cells and in nascent PGCs during specification of the germline (Yamaji et al., 2008). Loss of *Prdm14* in mice causes lack of germ cells by mid-gestation and subsequent infertility (Yamaji et al., 2008). Mechanistic analyses using mouse pluripotent stem cells have demonstrated the important role of *Prdm14* in PGC fate induction, epigenetic reprogramming, and acquisition of naïve pluripotency (Grabole et al., 2013; Leitch et al., 2013; Mallol et al., 2019; Nakaki et al., 2013; Okashita et al., 2016; Yamaji et al., 2013).

Here, we genetically modified the rat *Prdm14* locus. We introduce a fluorescent reporter, *histone H2B* fused to *Venus* (*H2BVenus*), in the *Prdm14* locus to monitor and purify developing rat PGCs. We also generate *Prdm14*-deficient rats, which reveal a conserved function of *Prdm14* among rodents.

[1]Section of Mammalian Transgenesis, Center for Genetic Analysis of Behavior, National Institute for Physiological Sciences, Okazaki, 444-8787 Aichi, Japan. [2]Department of Physiological Sciences, The Graduate University of Advanced Studies, Okazaki, 444-8787 Aichi, Japan. [3]Department of Embryology, Nara Medical University, Kashihara, 634-0813 Nara, Japan. [4]Department of Bioscience, Tokyo University of Agriculture, Setagaya-ku, 156-8502 Tokyo, Japan. [5]Division of Stem Cell Therapy, Institute of Medical Science, The University of Tokyo, Minato-ku, 108-8639 Tokyo, Japan. [6]Institute for Stem Cell Biology and Regenerative Medicine, Department of Genetics, Stanford University School of Medicine, Stanford, CA 94305, USA.
*These authors contributed equally to this work
‡These authors contributed equally to this work

§Author for correspondence (mhirarin@nips.ac.jp)

T.K., 0000-0001-8019-0008; H.K., 0000-0003-3800-4691; T.G., 0000-0002-0081-3357; M.H., 0000-0002-1059-5883

**Received 10 August 2019; Accepted 15 January 2020**

Development (2020) 147, dev183798. doi:10.1242/dev.183798

## RESULTS AND DISCUSSION

### Tracing germline development in *Prdm14-H2BVenus* knock-in rats

To visualize the expression pattern of *Prdm14* in rats, we replaced exons 1-4 of the endogenous *Prdm14* with the *H2BVenus* fluorescent gene in rat embryonic stem cells (ESCs) via homologous recombination (Fig. 1A, Fig. S1A,B). All *Prdm14-H2BVenus* heterozygous knock-in rat ESC lines homogeneously expressed H2BVenus (Fig. S1C,D), akin to mouse ESCs cultured under defined conditions (Yamaji et al., 2013). We generated chimeric rats by

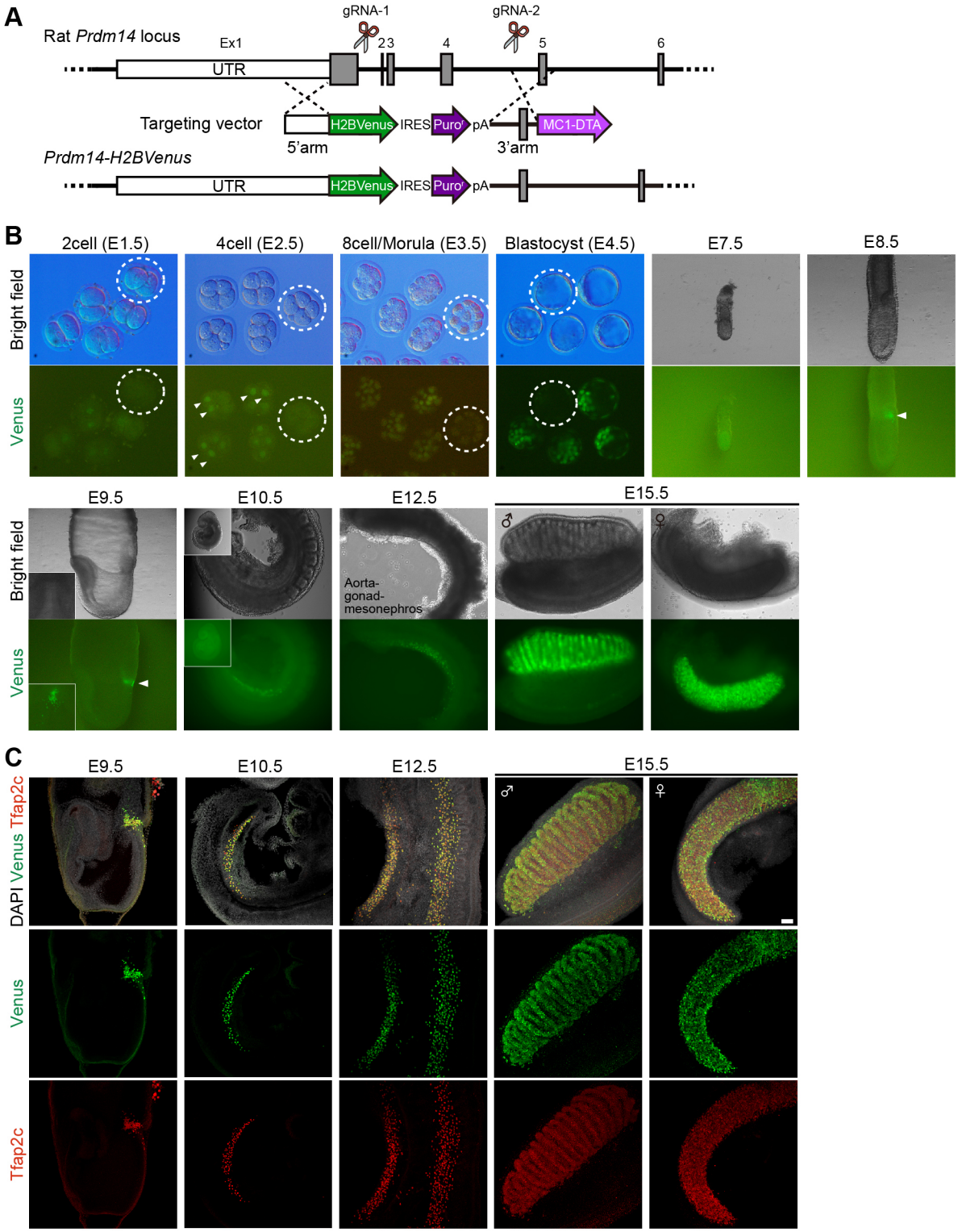


**Fig. 1. Expression pattern of *Prdm14-H2BVenus* during embryo development in rats.** (A) Targeting strategy for *Prdm14-H2BVenus* knock-in rats. (B) Expression of *Prdm14-H2BVenus* during pre- and post-implantation rat development. Dashed lines in two-cell to blastocyst panels indicate wild-type embryos. Arrowheads indicate faint fluorescent signals for H2BVenus. (C) Whole-mount immunostaining of *Prdm14*$^{+/HV}$ embryos. Scale bar: 100 µm.

Development (2020) 147, dev183798. doi:10.1242/dev.183798

injecting a knock-in rat ESC line into wild-type rat blastocysts. Crossing the chimeras with wild-type rats yielded heterozygous (*Prdm14*$^{+/HV}$) rats obtained through germline transmission of the ESC line (Fig. S1E). We then analyzed the expression pattern of *Prdm14-H2B Venus* in the embryos and fetuses that were obtained by crossing the *Prdm14*$^{+/HV}$ rat with wild-type rats.

During preimplantation development, two-cell-stage embryos started to express *H2BVenus* in the nucleus and subsequently maintained expression until the blastocyst stage (Fig. 1B). In mice, *Prdm14* is heterogeneously expressed in four-cell-stage embryos, and might be involved in promoting lineage allocation towards the inner cell mass (Burton et al., 2013). In agreement, some blastomeres in four-cell-stage rat embryos showed higher *H2BVenus* expression than others (Fig. 1B, arrowheads in 4cell). Moreover, the inner cell mass containing pluripotent cells in the blastocyst at embryonic day (E) 4.5 showed a brighter H2BVenus signal than the surrounding trophectoderm layer (Fig. 1B, blastocyst). Although further functional validation is necessary, the role of *Prdm14* in preimplantation development might be well-conserved within rodents.

After implantation, although fluorescence was almost undetectable prior to gastrulation (~E7.5), a cluster of cells at the posterior epiblast adjacent to the extra-embryonic ectoderm in gastrulating E8.5 embryos faintly, but specifically, showed expression of H2BVenus (Fig. 1B, arrowhead in E8.5). The number of H2BVenus$^{+}$ cells increased at E9.5. The expression pattern of H2BVenus in whole-mount immunostained E9.5 embryos closely correlated with that of Tfap2c, an essential PGC specifier (Weber et al., 2010), suggesting that H2BVenus specifically marks PGCs (Fig. 1C). H2BVenus$^{+}$ PGCs expressing Tfap2c migrated along the hindgut at E10.5-11.5 and reached the gonadal region at around E12.5 (Fig. 1B,C). In gonads, rat PGCs expressing Tfap2c as well as Ddx4 progressively expanded by E15.5, which is when the gonads show obvious morphological difference between sexes (Fig. 1B,C, Fig. S2). At later stages, the expression level of H2BVenus and the number of H2BVenus$^{+}$ cells in the gonadal germ cells gradually declined until birth, and germ cells in testes or ovaries of postnatal day 8 rats did not show any expression (Fig. S2). Collectively, inserting the *H2BVenus* gene into the rat *Prdm14* locus reveals its unique expression pattern, in pluripotent cells during preimplantation development and in PGCs during post-implantation development.

### Specification of rat PGCs in peri-gastrulating embryos

We next examined the timing of PGC specification in rats based on H2BVenus fluorescence in peri-gastrulating embryos (~E7.75-8.75). We used morphological features to stage embryos (Fig. S3A) and whole-mount immunostaining for Oct3/4 (also known as Pou5f1) (epiblast) and brachyury (T) (primitive streak/mesoderm) to define developmental timing accurately.

At the pre-streak stage (E7.75), the epiblast uniformly expressed Oct3/4 but T was not detectable (Fig. 2A, E7.75). However, at the early streak stage (E8.0), the posterior epiblast started to express T, indicating onset of gastrulation (E8.0; Fig. 2A). Notably, a few T$^{+}$ cells showed faint expression of Prdm14-H2BVenus (Fig. 2A, arrowheads in insets of E8.0 embryo), suggesting that nascent PGCs in rat might be specified from T$^{+}$ cells at this stage. The number of H2BVenus$^{+}$ nascent PGCs among T$^{+}$ cells at the posterior epiblast gradually increased with elongation of the primitive streak at E8.25, defined as the mid-streak stage (Fig. 2A, E8.25). Then, at late primitive streak no bud (LSOB) stage (E8.5), the nascent PGCs formed an obvious cluster (Fig. 2A, E8.5), as shown in Fig. 1B. At E8.75, when the allantois bud appears and the amnion closes, the size of the cluster increased whereas T expression declined, indicating suppression of somatic genes (Fig. 2A,B, E8.75). The presence of H2BVenus$^{+}$ cells distant from the cluster might reflect dynamic movement of rat PGCs, as has been observed in mice (McDole et al., 2018).

We next examined expression of the tripartite core PGC specifiers *Prdm1*, *Tfap2c* and *Prdm14* (*H2BVenus*), which are sufficient to induce PGC fate in the mouse epiblast (Magnúsdóttir et al., 2013; Nakaki et al., 2013). At E8.5 (LSOB), cells at the posterior epiblast expressed either Prdm14-H2BVenus and/or Prdm1 but not Tfap2c, whereas the extra-embryonic ectoderm strongly expressed Tfap2c (Fig. 2C, *Prdm14*$^{+/HV}$). The presence of either Prdm1 or Prdm14 single-positive cells suggests that T might induce these transcription factors independently, as in mice (Aramaki et al., 2013). At early to late head fold stage (E-LHF: E9.5), PGCs expressed all three regulators concomitantly, suggesting that these factors have established the network for germ cell fate (Fig. 2D, *Prdm14*$^{+/HV}$). *Tfap2c* is a downstream target of Prdm1 and Prdm14 (Cheetham et al., 2018; Kurimoto et al., 2015). This chronological order of key transcription factor expression is reflected in our immunostaining with the reporter in rat.

We also checked for expression of the pluripotency genes *Oct3/4* and *Sox2*, both of which are important for the maintenance of PGCs in mice (Campolo et al., 2013; Okamura et al., 2008). At E8.5 (LSOB), Oct3/4 expression was slightly reduced in H2BVenus$^{+}$ nascent PGCs as well as surrounding T$^{+}$ cells, whereas Sox2 expression is absent and restricted to the anterior epiblast (E8.5; Fig. 2A, Fig. S3B). At E9.5 (E-LHF), H2BVenus$^{+}$ PGCs co-express both *Oct3/4* and *Sox2*, as well as *Nanog*, another core pluripotency gene (Fig. S6C), suggesting that, like in mouse, rat PGCs also upregulate a pluripotency-associated gene program (*Prdm14*$^{+/HV}$; Fig. 2D, E9.5; Fig. S3B).

### Disruption of rat *Prdm14* causes defects in PGC specification and leads to infertility

Because *Prdm14* is the earliest marker for nascent PGCs, we next analyzed its function in rats. *Prdm14*-deficient rats were obtained by crossing *Prdm14*$^{+/HV}$ with *Prdm14*$^{+/mut}$, another mutant line with a deletion in exon 1-4 like the *Prdm14*$^{+/HV}$ (Fig. S1F,G). The use of two lines allows us to compare the expression level of H2BVenus precisely in both heterozygous and homozygous mutants, as both have a single copy of the *H2BVenus* gene.

In *Prdm14*$^{mut/HV}$ embryos at E8.5 (LSOB), we detected similar numbers of Prdm14-H2BVenus$^{+}$ nascent PGCs as were observed in *Prdm14*$^{+/HV}$ embryos (Figs 2C and 3B). The nascent PGCs expressed Prdm1 even in the absence of Prdm14 in *Prdm14*$^{mut/HV}$ embryos (Fig. 2C) concordant with *Prdm1* expression being independent of *Prdm14*. In contrast, at E9.5 (EHF-LHF), H2BVenus expression in *Prdm14*$^{mut/HV}$ embryos was not upregulated as it is in *Prdm14*$^{+/HV}$ embryos (Fig. 2D). More importantly, the faint H2BVenus$^{+}$ cells did not express *Prdm1*, *Tfap2c* or *Sox2* at either the protein or mRNA level (*Prdm14*$^{mut/HV}$; Figs 2D and 3A). The number of H2BVenus$^{+}$ cells was unchanged from E8.5, which is in contrast to heterozygous or wild-type embryos in which the PGC numbers increased by 3-fold within 1 day (Fig. 3B). Thus, loss of *Prdm14* leads to failure in activation and/or maintenance of key regulators that are essential for the PGC fate as well as subsequent re-acquisition of pluripotency genes. Notably, even in the absence of *Prdm14*, mouse PGCs delay but retain the expression of several germ cell markers as well as pluripotency genes at the transcript level (Grabole et al., 2013; Shirane et al., 2016; Yamaji et al., 2008). Although further careful analysis matching the reporter and developmental stage between

Development (2020) 147, dev183798. doi:10.1242/dev.183798

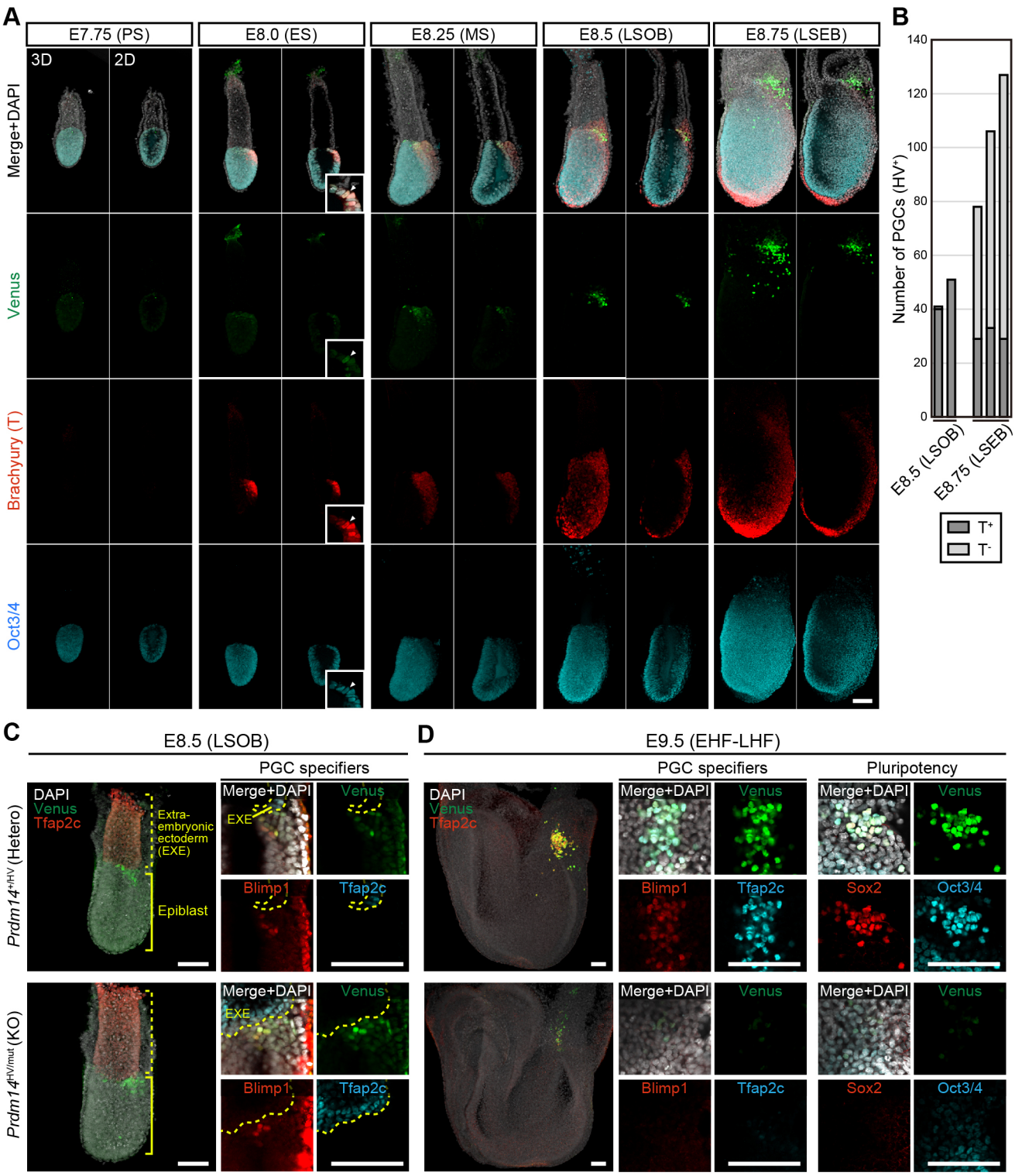


**Fig. 2. Monitoring PGC specification in rats.** (A) Staging of *Prdm14*$^{+/HV}$ peri-gastrulating embryos by whole-mount immunostaining. Insets show T$^{+}$ posterior epiblast. Arrowheads indicate a faint Prdm14-H2BVenus$^{+}$ rat PGC. (B) Quantification of T$^{+}$ cells in Prdm14-H2BVenus$^{+}$ rat PGCs. (C) Expression of core PGC specifiers in E8.5 embryos. Dashed lines delineate extra-embryonic ectoderm (EXE). (D) Expression of core PGC specifiers and pluripotency genes in E9.5 embryos. EHF, early head fold stage; ES, early streak stage; LHF, late head fold stage; LSEB, late-streak, early bud stage; LSOB, late-streak, no bud stage; MS, mid-streak stage; PS, pre-streak stage. Scale bars: 100 µm.

mouse and rat are necessary, *Prdm14* might regulate PGC specification more stringently in rats than in mice.

As a result of the collapse in the pre-migratory PGCs, gonads of *Prdm14*-deficient embryos at E15.5 completely lost germ cells, whereas the supporting somatic cells were entirely normal (Fig. 3C, Fig. S4). Although the testes and ovaries at postnatal day 1 appeared similar between the knockout and wild type, they were smaller in young (4 weeks) and adult (13 weeks or 18 weeks) rats due to the

Development (2020) 147, dev183798. doi:10.1242/dev.183798

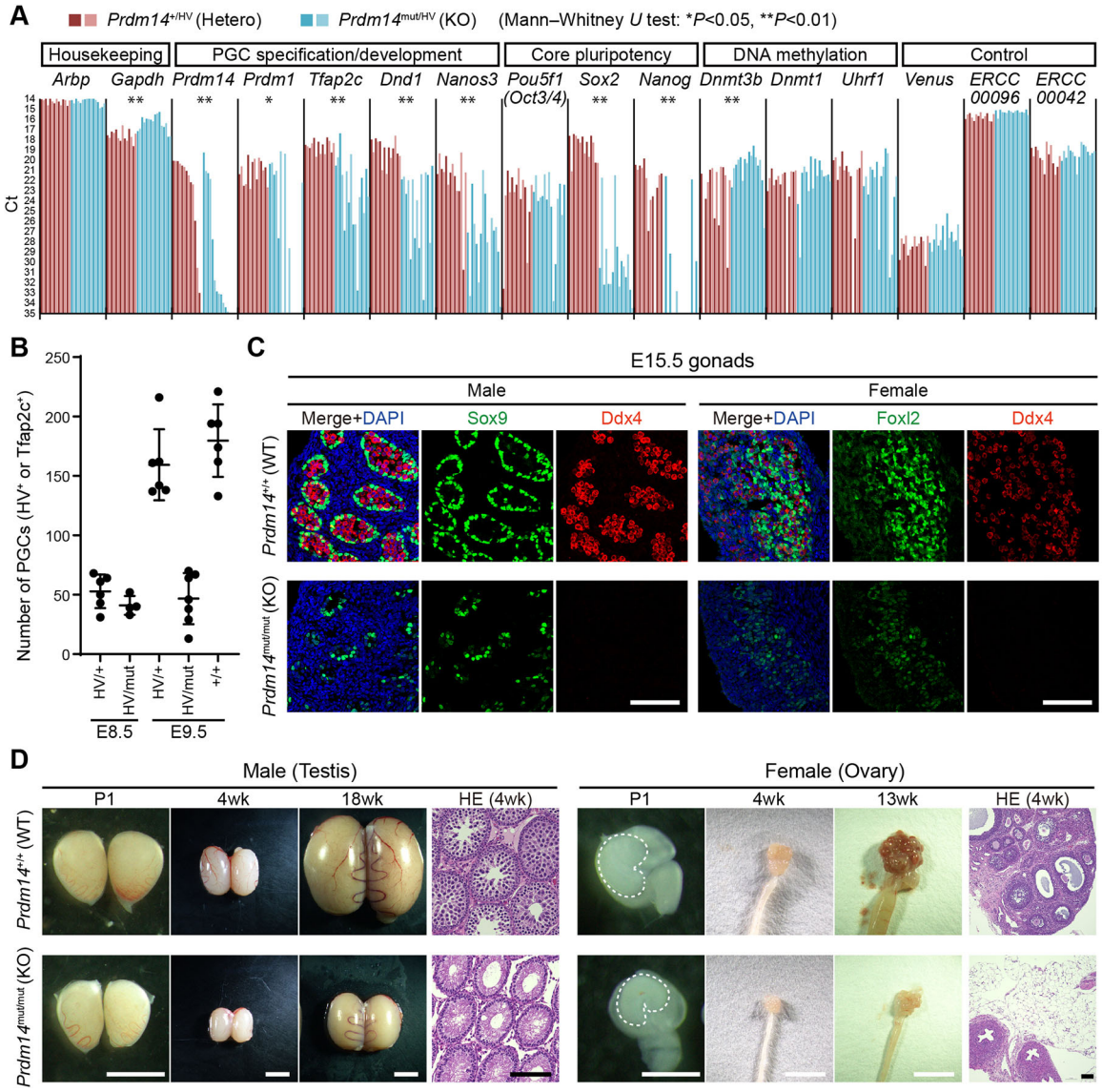


**Fig. 3. Analysis of *Prdm14*-deficient rats.** (A) Single cell RT-qPCR analysis of rat PGCs. (B) Number of PGCs counted from whole-mount immunostained embryos. Prdm14-H2BVenus$^{+}$ PGCs in *Prdm14*$^{+/HV}$ and *Prdm14*$^{mut/HV}$, Tfap2c$^{+}$ PGCs in *Prdm14*$^{+/+}$ were counted, respectively. Error bars represent s.d. (C) E15.5 gonadal cryosection immunostaining. Scale bars: 100 µm. (D) Testes and ovaries from neonates to adults and paraffin-embedded sections stained with Hematoxylin and Eosin (HE). Scale bars: 2 mm (P1); 5 mm (4, 13 and 18 weeks); 100 µm (HE).

lack of germ cells (Fig. 3D, Fig. S4). Therefore, loss of *Prdm14* in rats causes infertility both in males and females like in *Prdm14*-deficient mice (Yamaji et al., 2008).

### Transcriptional dynamics during rat PGC development

To obtain further information on rat PGCs at each developmental stage, we purified PGCs at various stages and used RNA sequencing (RNA-seq) to investigate changes to the transcriptome during development. We collected H2BVenus$^{+}$ cells at E9.5 (early PGCs), E10.5 and E11.5 (migratory PGCs), and E12.5 and E15.5 (gonadal PGCs) (Fig. S5B). In addition to the PGC samples, we also isolated the post-implantation epiblast at E7.25 and E7.75 as reference, because the epiblast differentiates into all germ layers including the germline (Fig. S5A).

A heat map of the correlation coefficients shows high correlation between each replicate and cell type (Fig. S5C). Hierarchical clustering of 8966 detectable genes resulted in two distinct clusters consisting of the pluripotent epiblast and developing PGCs (Fig. S5D). In the principal component analysis (PCA), PC1 reflects dynamic changes in mitochondrial gene expression during PGC development (Fig. S5E,G) as shown for mice and human (Cree et al., 2008; Floros et al., 2018), and the PC2/PC3 scatterplot nicely reflects a temporal trajectory from epiblast to PGCs (Fig. 4A, Fig. S5E). From the PCA, we extracted positively and negatively expressed gene sets correlated with the PC loading (Fig. S5F) and performed K means clustering analysis using the gene sets (K=9) (Fig. 4B). Cluster 1/2/3 genes, upregulated in the epiblast samples, are enriched in gene ontogeny (GO) terms related to morphological and metabolic pathways of post-implantation epiblast (Fig. 4B, right). Importantly, *de novo* DNA methyl-transferase genes (*Dnmt3a*, *Dnmt3b* and *Dnmt3l*) were highly enriched in Cluster 1/2/3, and dramatically downregulated in the PGCs (Fig. 4B,C). In addition, expression of *Uhrf1*, which is essential for maintenance of DNA methylation, was also reduced in PGCs at E9.5 compared with the epiblast (Fig. 4C). Subsequently, methylation-sensitive germ cell-related genes, such as *Ddx4*, *Dazl* and *Mael*, were progressively upregulated (Fig. S6C),

Development (2020) 147, dev183798. doi:10.1242/dev.183798

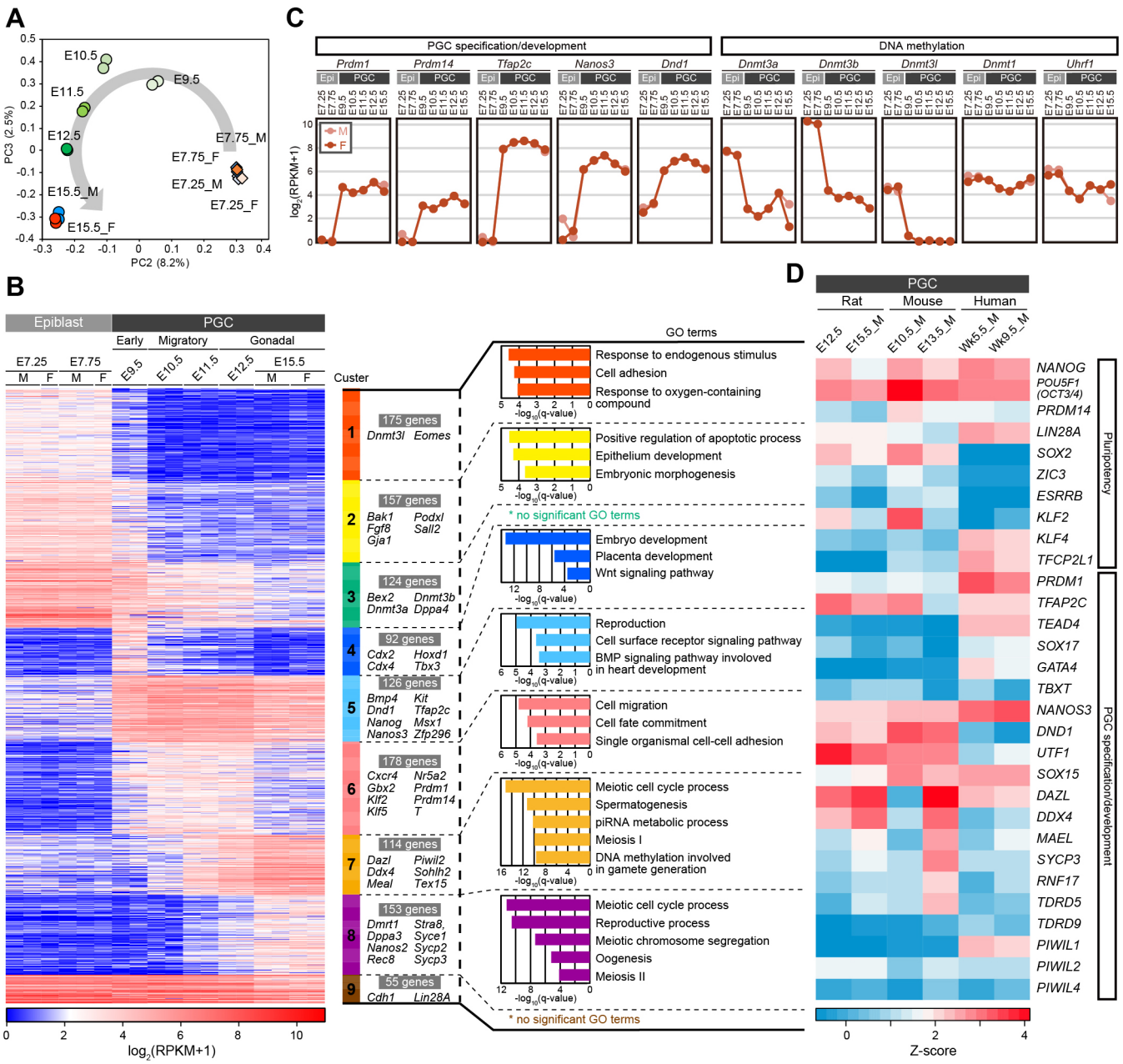


**Fig. 4. Transcriptome dynamics in developing rat PGCs.** (A) PCA of PGC lineage for all expressed genes (8966 genes). F, female; M, male. (B) Heat map of significant genes (1174 genes), which were divided into nine clusters by K-means analysis. Representative genes in each cluster and enrichments of the gene ontology (GO) terms are shown next to the heat map. (C) Expression changes of representative genes. Epi, epiblast. (D) Heat map of key PGC genes among mouse, rat and human PGCs.

suggesting that rat PGCs at E9.5 initiate extensive epigenetic reprogramming. Cluster 4, transiently upregulated in early PGCs at E9.5, contained 'embryo development' genes including some mesoderm markers (*Cdx2*, *Cdx4*, *Hoxd1* and *Tbx3*), which are suppressed by the germ cell program at later stages (Fig. 4B, Fig. S6C). Cluster 5/6 contained modestly (Cluster 5) or abundantly (Cluster 6) expressed key germ cell-related genes (*Prdm1*, *Prdm14*, *Tfap2c*, *Nanos3*, *Dnd1*, *Nr5a2* and *Zfp296*), all transcription factors crucial for specification and/or maintenance of PGCs in mice and the other species (Fig. 4B,C) (Bleckwehl and Rada-Iglesias, 2019; Sybirna et al., 2019b). Cluster 7/8 contained highly expressed gametogenesis and meiosis genes associated with late PGCs (Fig. 4B). Taken together, transcriptome analysis of purified rat PGCs uncovers gene sets that mark key events and transition points during PGC specification and subsequent development.

Finally, to reveal conserved/species-specific gene expression patterns in PGCs, we performed a cross-species comparison among mouse, rat and human early/late gonadal PGCs. Hierarchical clustering of 980 homologous genes revealed separate clustering depending on the species (Fig. S6A). A heat map of correlation coefficients shows that each developmental stage of PGCs is highly correlated particularly within rodents (Fig. S6B). A 1- to 2-day lag in gestation period between mouse and rat reflects the difference in PGC development timeline.The expression pattern of key PGC genes exhibits some conservation across the mammals but there are significant differences between rodents and human (Fig. 4D).

Development (2020) 147, dev183798. doi:10.1242/dev.183798

*Sox17*, a key transcriptional regulator of PGCs in non-rodent mammals (Irie et al., 2015; Kobayashi et al., 2017), is almost absent in mouse and rat gonadal PGCs, whereas it is temporarily upregulated in early PGCs in rats (Fig. S5F) and mice (Yabuta et al., 2006). Furthermore, expression patterns of pluripotency genes such as *Sox2*, *Klf4* and *Tfcp2l1* also show a similar divergence, confirming that the PGC program is highly conserved between rat and mice.

In summary, by genetically modifying a core germ cell specifier, *Prdm14*, in rats, we obtained a faithful reporter line to monitor and purify developing rat PGCs and a knockout line to reveal its crucial function in PGC fate. Overall, the dynamics and transcriptional regulatory network of PGCs are well conserved within the rodents, albeit delayed in rats due to a difference in gestation periods. However, some differences might impact the regulation of pluripotency and germline development. For instance, although lack of *Prdm14* causes infertility in both mouse and rat, the influence on PGC specification might be more severe in rat than in mouse. As naïve pluripotent stem cells in rats can be maintained only under very stringent conditions (Buehr et al., 2008; Buehr et al., 2003; Li et al., 2008), rat PGCs might also be sensitive to changes in the transcriptional regulatory network. A recent work demonstrated that *PRDM14* is crucial for human PGC specification and activates distinct transcription programs in mouse and human (Sybirna et al., 2019a preprint), playing context-dependent roles. Similar analysis of *Prdm14* function in rats would extend our understanding of PGC networks across species.

Further investigation in rats using the models we have generated, and comparative studies across species will reveal the conserved principles of germline development, which will be informative for the establishment of a widely applicable *in vitro* system for reconstituting the rat germline cycle.

## MATERIALS AND METHODS

### Animals

Crlj:WI rats (RGD ID: 2312504) were purchased from Charles River Laboratories Japan (Kanagawa, Japan). C57BL/6N mice were purchased from Clea Japan (Tokyo, Japan). All experiments were performed in accordance with the animal care and use committee guidelines of the National Institute for Physiological Sciences and Tokyo University of Agriculture.

### Generation of *Prdm14-H2BVenus* rats

For construction of targeting vector, 5′ and 3′ homology arms amplified from genomic DNA of rat ESCs (WDB/Nips-ES1/Nips, RGD ID: 10054010) (Hirabayashi et al., 2012), H2BVenus-IRES-Puro$^r$ amplified from prRosa26-H2BVenus-IRES-Puro$^r$ vector (Kobayashi et al., 2012), and MC1-DTA cassette amplified from a MC1-DTA vector were assembled and inserted into pBluescript KS(+) (Stratagene) with an in-fusion HD cloning kit (Takara Bio). For efficient gene targeting, we used the CRISPR/Cas9 system. Guide RNAs targeting around the start codon sequence of rat *Prdm14* genes (A: 5′-caccgGGTCTCGCGAGAAGGCGATA-3′, 5′-aaac-TATCGCCTTCTCGCGAGACCc-3′; B: 5′-caccgACATTCGTCAAGTA-GACGAG-3′, 5′-aaacCTCGTCTACTTGACGAATGTc-3′) were cloned into eSpCas9(1.1) (Addgene plasmid #71814).

For gene targeting, undifferentiated rat ESCs (WDB/Nips-ES1/Nips, RGD ID: 10054010) were maintained on mitomycin-C-treated mouse embryonic fibroblasts (MEFs) in N2B27 medium containing 1 µM PD0325901 (Axon, Groeningen, The Netherlands), 3 µM CHIR99021 (Axon) and 1000 U/ml of rat leukemia inhibitory factor (Millipore). To introduce the vectors into rat ESCs, we carried out reverse transfection using Lipofectamine 2000 (Thermo Scientific) as described before (Kobayashi et al., 2017). In brief, 2×10e5 rat ESCs were suspended in 100-200 µl of Opti-MEM (Thermo Scientific) containing the targeting vector, CRISPR/Cas9 vector, and Lipofectamine 2000 (Thermo Scientific), and were incubated for 5 min at room temperature. Then, rat ESCs were seeded onto four-drug resistant (DR4) MEFs and 48 h later, 0.5 µg/ml puromycin (Sigma-Aldrich) was added to the culture medium for selection. After the selection, puromycin-resistant and H2BVenus$^+$ rat ESC colonies were picked. Correct targeting was confirmed by PCR using primers shown in Fig. S1A and Table S1 and a representative result is shown in Fig. S1B.

For making chimeric rats and obtaining germline transmission, we performed blastocyst injection of targeted rat ESCs. Rat blastocysts were collected in mR1ECM medium from oviduct and uterus of rats 4.5 days post-coitum (dpc). For micro-manipulation, rat ESCs were trypsinized and suspended in rat ESC medium. A piezo-driven micro-manipulator (Prime Tech, Tokyo, Japan) was used to drill zona pellucida and trophectoderm under the microscope and eight rat ESCs were introduced into blastocyst cavities near the inner cell mass. After the injection, the blastocysts were transferred into the uterus of pseudopregnant recipient Wistar rats (3.5 dpc).

### Generation of *Prdm14* mutant rats

For efficient and rapid generation of *Prdm14* mutant rats, we performed electroporation to introduce CRISPR/Cas9 system into fertilized rat embryos. Ribonucleic complexes composed of 100 ng/µl crRNA (the target is the same with A and B in *Prdm14-H2BVenus* rats), 200 ng/µl tracrRNA and 200 ng/µl Cas9 protein (all products were purchased from IDT) were prepared according to the manufacturer's protocol. Rat pronuclear stage embryos were collected in mKRB medium from the oviducts of rats 0.5 days dpc. Electroporation was carried out using NEPA21 (Nepagene) according to the manufacturer's protocol. After electroporation, the embryos underwent follow-up culture for 1 day in mKRB medium and were transferred into the oviduct of pseudopregnant recipient Wistar rats (0.5 dpc). Large deletion mutants were judged by PCR and subsequent Sanger sequencing. Of 13 mutant lines, we used two mutant lines (Mutant-3 and -10) with identical phenotypes for the following experiments (Fig. S1F,G).

### Collection of rat epiblast and PGCs

For isolating rat epiblast (*Prdm14*$^{+/HV}$) at E7.25 and E7.75, the ectoplacental cone and extra-embryonic ectoderm was mechanically cut off. Then, the visceral endoderm surrounding the epiblast was removed by enzymatic treatment using 1.0 mg/ml collagenase type IV (Worthington Biochemical Corporation), 1.0 mg/ml dispase (FUJIFILM Wako, Osaka, Japan) and 0.3 mg/ml hyaluronidase (Sigma-Aldrich) (Rivera-Pérez et al., 2007) for 3-5 min at 37°C followed by repeated pipetting with a glass capillary tube. For purifying rat PGCs from *Prdm14*$^{+/HV}$ rat embryos, the embryonic tissues indicated in Fig. S5A,B were dissected and trypsinized using 0.25% trypsin/EDTA for 5 min at 37°C. H2BVenus$^+$ rat PGCs were collected with the SH800 cell sorter (Sony). The genotype of the embryos was determined by H2BVenus fluorescence or PCR using ectoplacental cone and/or extra-embryonic ectoderm.

### Immunostaining of rat embryos and tissues

Embryos were fixed in 4% paraformaldehyde for 10-30 min at room temperature (RT) or from 4 h to overnight at 4°C depending on the stages. For cryosections, the fixed embryos were embedded in OCT compound. Each sample was incubated with primary antibodies for 1-2 h at RT or overnight at RT or 4°C, and then with fluorescent-conjugated secondary antibodies with DAPI (FUJIFILM Wako) for 1 h at RT or overnight at 4°C. Antibodies used are listed on Table S2. For embryos, the samples were cleared with CUBIC1/2 or CUBIC2 alone according to a published protocol (Kubota et al., 2017). The embryos and cryosections were observed under a confocal laser-scanning microscope (Nikon A1Rsi).

### Single cell gene expression analysis

cDNAs of single rat PGCs were amplified following a previously described method with a minor modification as follows (Kurimoto et al., 2006). For cell collection, *Prdm14*$^{+/HV}$ and/or *Prdm14*$^{mut/HV}$ embryos were obtained by crossing *Prdm14*$^{+/HV}$ and *Prdm14*$^{+/mut}$ rats. By using the SH800 cell sorter, H2BVenus$^+$ cells in embryos at early head fold stage (E9.5) were collected in a 50 µl droplet of PBS containing 0.5% polyvinyl alcohol on the cover of a 96-well tissue culture plate (IWAKI). Then, the cells were picked up into

Development (2020) 147, dev183798. doi:10.1242/dev.183798

0.5 ml PCR tubes (Life Technologies) containing 4.5 µl of cell-lysis buffer with ERCC RNA spike-in Mix (Thermo Fisher) (Nakamura et al., 2015), using a mouth pipette as described (Kurimoto and Saitou, 2011), and were snap frozen in liquid nitrogen. The frozen cells were stored in dry ice or at −80°C until use. Genotypes of the embryos were judged by PCR using the ectoplacental cone as described above. We decided to compare gene expression levels of cells from littermate embryos. Just before use, the frozen cells were thawed on ice, and single cell cDNA amplification was performed as described (Kurimoto et al., 2006), with a minor modification. In brief, for the 20-cycle PCR amplification step after the second-strand synthesis, we added 1 µl of 0.375 µg/µl V1(dT)24 primer to each reaction tube (final concentration of 20 ng/µl), instead of 19 µl of a mixture containing ExTaq buffer, dNTPs, V1(dT)24 primer and ExTaq, which was used in the original protocol (Kurimoto et al., 2006). Expression levels of selected genes were analyzed by real-time PCR using the primers shown in Table S3. Samples with extremely low/high levels of spike RNAs (ERCC) and/or housekeeping genes [*Arbp* (*Rplp0*), *Gapdh*] were eliminated from the analysis as outliers.

### Preparation of rat RNA-sequencing libraries

Total RNA was extracted using the PicoPure RNA Isolation Kit (Thermo Fisher Scientific) according to the manufacturer's protocols. Two hundred picograms of total RNA were reverse transcribed using SMART-Seq v4 Ultra Low Input RNA Kit (Takara Bio). The synthesized cDNA was amplified with 15 cycles of PCR. Each of the cDNA libraries were indexed and prepared for Illumina sequencing using KAPA Hyper Prep Kit (Kapa Biosystems) with 13 cycles of PCR. The RNA-seq libraries were quantified by qPCR using KAPA Library Quantification Kit (Kapa Biosystems). All libraries were mixed and subjected to single-end 75 bp sequencing on NextSeq 500 system (Illumina) using High Output Kit v2. Basecalls were performed using NextSeq 500/550 RTA software (v. 2.4.11). FASTQ files were generated using bcl2fastq (v. 2.18.0.12).

### Mouse PGC RNA-sequencing library preparation

Mouse male and female PGCs at E10.5 were isolated and subjected to RNA-sequencing preparation. Briefly, heterozygous *Pou5f1-ΔPE-GFP* mouse embryos (C57BL/6N background) were recovered at E10.5, and the sex was distinguished based on PCR amplification of *Zfy* gene (Kobayashi et al., 2013). GFP-positive PGCs were sorted by flow cytometry. Purified 500 pg to 1 ng of total PGC RNA were used to generate cDNA libraries with 12 cycles of PCR amplification using the SMARTer v4 Ultra Low Input RNA Kit. Pre-amplified cDNA was fragmented into 200-bp fragments using an S2 sonicator (Covaris) and then used to construct sequencing libraries with 15 cycles of PCR using a NEBNext Ultra DNA Library Prep Kit (New England BioLabs). After qPCR quantification using the KAPA Library Quantification Kit, all libraries were mixed and subjected to single-end 50 bp sequencing on HiSeq 2500 system (Illumina). Basecalls were performed using HiSeq RTA software (v. 1.17.20). FASTQ files were generated using bcl2fastq (v. 2.17.1.14). Raw sequence data of E13.5 male and female PGCs was downloaded from DDBJ (accession: DRA003597) (Sakashita et al., 2015).

### Bioinformatics analysis

For processing the rat and mouse RNA-seq data, the first three bases were trimmed out from raw reads using FASTX Toolkit 0.0.13.2. Trimmed reads were further quality-trimmed using the Cutadapt v. 1.14 program with the following configurations: trimming the primer 'Clontech SMART CDS Primer II A: AAGCAGTGGTATCAACGCAGAGTAC'; minimal base quality: 20; minimal read length after trimming: 35 nt. RNA-seq reads were aligned to the rat (rn6) or mouse (mm10) genome assembly using TopHat2 (v. 2.1.0) with bowtie2 (v. 2.3.4.1). Cufflinks version 2.2.1 program together with Ensembl gene annotation (rn6, 32545 genes; mm10, 46073 genes) were used to assemble transcripts and estimate their abundances. The read densities [reads per kilobase of transcript per million reads (RPKM)] were converted to the $\log_2$ (RPMK+1) scale ($\log_2$ expression level), and averaged among the biological replicates.

For PCA and GO analysis, rat genes showing maximum $\log_2$ (RPKM+1) values >3 in at least one replicate were selected (8966 genes). Hierarchical clustering was performed based on Ward's method using 'hclust' function of R package. The PCA was performed using the 'prcomp' function of the R package without scaling. Significant differentially expressed genes (DEGs) were defined as genes showing a more than 2 s.d. radius of scaled PC2 and PC3 values (1174 genes). Significant genes were grouped into K-means clusters (K=9) using the 'kmeans' function of R package. GO analysis was performed using DAVID (v. 6.8).

For cross-species comparison between human, raw sequence data of human PGCs was downloaded from NCBI: SRP057098 (PRJNA280935). Raw reads were quality- and adaptor-trimmed using the Trim_galore v. 0.6.4 program with the following configurations: minimal base quality: 25; minimal read length after trimming: 35 nt. RNA-seq reads were aligned to the hg38 genome assembly using TopHat2 (v. 2.1.0) with bowtie2 (v. 2.3.4.1). Cufflinks version 2.2.1 program together with Ensembl gene annotation (hg38, 60594 genes) were used to assemble transcripts and estimate their abundances. The RPKM values were converted to the $\log_2$ (RPMK+1) scale, and averaged across biological replicates. For comparison, one-to-one orthologous genes in the rat, mouse and human were listed using BioMart (Ensembl) with Z-score values. Orthologs of significant DEGs were selected (980 genes), and hierarchical clustering was performed using R package. Correlation coefficients between two variables (mouse/rat/human samples) were calculated using Excel.

#### Acknowledgements

We thank members of the Hirabayashi lab, particularly Keiko Yamauchi, Megumi Hashimoto and Naoko Niizeki for help with animals, and Minako Ohnishi for secretarial support. We thank Prof. Yayoi Obata, Prof. Tomohiro Kono and Dr Akihiko Sakashita of Tokyo University of Agriculture for their help in preparing mouse PGCs and valuable discussion regarding data analysis. We also thank Dr Roopsha Sengupta for editing and providing critical input to the manuscript. We thank the Spectrography and Bioimaging Facility, NIBB Core Research Facilities for technical support.

#### Competing interests

The authors declare no competing or financial interests.

#### Author contributions

Conceptualization: T.K., H.K., K.K.; Methodology: T.K., H.K., T.G., T.T., M.O., H.I., R.T., F.Y., M.S., K.K., M.H.; Validation: T.K.; Formal analysis: T.K., H.K., T.G., T.T., K.K.; Investigation: T.K., H.K., T.G., T.T., M.O., R.T., F.Y., K.K.; Resources: T.K., H.K., T.G., T.T., M.O., R.T., F.Y., K.K.; Data curation: H.K., T.T.; Writing - original draft: T.K.; Writing - review & editing: T.K.; Visualization: T.K., H.K., T.T.; Supervision: T.K., H.N., K.K.; Project administration: T.K.; Funding acquisition: T.K., H.N., M.H.

#### Funding

This work was supported by grants from Grant-in-Aid for Scientific Research from the Japan Society for the Promotion of Science (18H02367 to M.H. and T.K.; 18H05548 to T.K.; 18H05544 to T.K. and K.K.), and the Japan Agency for Medical Research and Development (LEAP-AMED; JP18gm0010002 to H.N. and M.H.). This work was partially supported by grants from AMED (JP18bm0704022 to T.K.), Cooperative Study Program (19-134) of National Institute for Physiological Sciences and the Cooperative Research Grant of the Genome Research for BioResource, NODAI Genome Research Center, Tokyo University of Agriculture.

#### Data availability

RNA-seq data have been deposited in Gene Expression Omnibus under accession number GSE135388 and DNA Data Bank of Japan under accession number DRA009457. All data included in the paper are listed in Table S4.

#### Supplementary information

Supplementary information available online at
http://dev.biologists.org/lookup/doi/10.1242/dev.183798.supplemental

#### Peer review history

The peer review history is available online at
https://dev.biologists.org/lookup/doi/10.1242/dev.183798.reviewer-comments.pdf

#### References

**Aitman, T. J., Critser, J. K., Cuppen, E., Dominiczak, A., Fernandez-Suarez, X. M., Flint, J., Gauguier, D., Geurts, A. M., Gould, M., Harris, P. C. et al.** (2008). Progress and prospects in rat genetics: a community view. *Nat. Genet.* **40**, 516-522. doi:10.1038/ng.147

**Aramaki, S., Hayashi, K., Kurimoto, K., Ohta, H., Yabuta, Y., Iwanari, H., Mochizuki, Y., Hamakubo, T., Kato, Y., Shirahige, K. et al.** (2013). A mesodermal factor, T, specifies mouse germ cell fate by directly activating germline determinants. *Dev. Cell* **27**, 516-529. doi:10.1016/j.devcel.2013.11.001

**Beaumont, H. M. and Mandl, A. M.** (1963). A quantitative study of primordial germ cells in the male rat. *J. Embryol. Exp. Morphol.* **11**, 715-740.

**Bleckwehl, T. and Rada-Iglesias, A.** (2019). Transcriptional and epigenetic control of germline competence and specification. *Curr. Opin. Cell Biol.* **61**, 1-8. doi:10.1016/j.ceb.2019.05.006

**Buehr, M., Nichols, J., Stenhouse, F., Mountford, P., Greenhalgh, C. J., Kantachuvesiri, S., Brooker, G., Mullins, J. and Smith, A. G.** (2003). Rapid loss of Oct-4 and pluripotency in cultured rodent blastocysts and derivative cell lines. *Biol. Reprod.* **68**, 222-229. doi:10.1095/biolreprod.102.006197

**Buehr, M., Meek, S., Blair, K., Yang, J., Ure, J., Silva, J., McLay, R., Hall, J., Ying, Q.-L. and Smith, A.** (2008). Capture of authentic embryonic stem cells from rat blastocysts. *Cell* **135**, 1287-1298. doi:10.1016/j.cell.2008.12.007

**Burton, A., Muller, J., Tu, S., Padilla-Longoria, P., Guccione, E. and Torres-Padilla, M.-E.** (2013). Single-cell profiling of epigenetic modifiers identifies PRDM14 as an inducer of cell fate in the mammalian embryo. *Cell Rep.* **5**, 687-701. doi:10.1016/j.celrep.2013.09.044

**Campolo, F., Gori, M., Favaro, R., Nicolis, S., Pellegrini, M., Botti, F., Rossi, P., Jannini, E. A. and Dolci, S.** (2013). Essential role of Sox2 for the establishment and maintenance of the germ cell line. *Stem Cells* **31**, 1408-1421. doi:10.1002/stem.1392

**Cheetham, S. W., Gruhn, W. H., van den Ameele, J., Krautz, R., Southall, T. D., Kobayashi, T., Surani, M. A. and Brand, A. H.** (2018). Targeted DamID reveals differential binding of mammalian pluripotency factors. *Development* **145**, dev170209. doi:10.1242/dev.170209

**Cree, L. M., Samuels, D. C., de Sousa Lopes, S. C., Rajasimha, H. K., Wonnapinij, P., Mann, J. R., Dahl, H.-H. M. and Chinnery, P. F.** (2008). A reduction of mitochondrial DNA molecules during embryogenesis explains the rapid segregation of genotypes. *Nat. Genet.* **40**, 249-254. doi:10.1038/ng.2007.63

**Encinas, G., Zogbi, C. and Stumpp, T.** (2012). Detection of four germ cell markers in rats during testis morphogenesis: differences and similarities with mice. *Cells Tissues Organs* **195**, 443-455. doi:10.1159/000329245

**Floros, V. I., Pyle, A., Dietmann, S., Wei, W., Tang, W. C. W., Irie, N., Payne, B., Capalbo, A., Noli, L., Coxhead, J. et al.** (2018). Segregation of mitochondrial DNA heteroplasmy through a developmental genetic bottleneck in human embryos. *Nat. Cell Biol.* **20**, 144-151. doi:10.1038/s41556-017-0017-8

**Gassei, K., Sheng, Y., Fayomi, A., Mital, P., Sukhwani, M., Lin, C.-C., Peters, K. A., Althouse, A., Valli, H. and Orwig, K. E.** (2017). DDX4-EGFP transgenic rat model for the study of germline development and spermatogenesis. *Biol. Reprod.* **96**, 707-719. doi:10.1095/biolreprod.116.142828

**Grabole, N., Tischler, J., Hackett, J. A., Kim, S., Tang, F., Leitch, H. G., Magnúsdóttir, E. and Surani, M. A.** (2013). Prdm14 promotes germline fate and naive pluripotency by repressing FGF signalling and DNA methylation. *EMBO Rep.* **14**, 629-637. doi:10.1038/embor.2013.67

**Hackett, J. A., Huang, Y., Günesdogan, U., Gretarsson, K. A., Kobayashi, T. and Surani, M. A.** (2018). Tracing the transitions from pluripotency to germ cell fate with CRISPR screening. *Nat. Commun.* **9**, 4292. doi:10.1038/s41467-018-06230-0

**Hayashi, K., Ohta, H., Kurimoto, K., Aramaki, S. and Saitou, M.** (2011). Reconstitution of the mouse germ cell specification pathway in culture by pluripotent stem cells. *Cell* **146**, 519-532. doi:10.1016/j.cell.2011.06.052

**Hayashi, K., Ogushi, S., Kurimoto, K., Shimamoto, S., Ohta, H. and Saitou, M.** (2012). Offspring from oocytes derived from in vitro primordial germ cell-like cells in mice. *Science* **338**, 971-975. doi:10.1126/science.1226889

**Hikabe, O., Hamazaki, N., Nagamatsu, G., Obata, Y., Hirao, Y., Hamada, N., Shimamoto, S., Imamura, T., Nakashima, K., Saitou, M. et al.** (2016). Reconstitution in vitro of the entire cycle of the mouse female germ line. *Nature* **539**, 299-303. doi:10.1038/nature20104

**Hirabayashi, M., Tamura, C., Sanbo, M., Goto, T., Kato-Itoh, M., Kobayashi, T., Nakauchi, H. and Hochi, S.** (2012). Ability of tetraploid rat blastocysts to support fetal development after complementation with embryonic stem cells. *Mol. Reprod. Dev.* **79**, 402-412. doi:10.1002/mrd.22043

**Irie, N., Weinberger, L., Tang, W. W. C., Kobayashi, T., Viukov, S., Manor, Y. S., Dietmann, S., Hanna, J. H. and Surani, M. A.** (2015). SOX17 is a critical specifier of human primordial germ cell fate. *Cell* **160**, 253-268. doi:10.1016/j.cell.2014.12.013

**Kemper, C. H. and Peters, P. W. J.** (1987). Migration and proliferation of primordial germ cells in the rat. *Teratology.* **36**, 117-124. doi:10.1002/tera.1420360115

**Kobayashi, T., Kato-Itoh, M., Yamaguchi, T., Tamura, C., Sanbo, M., Hirabayashi, M. and Nakauchi, H.** (2012). Identification of rat Rosa26 locus enables generation of knock-in rat lines ubiquitously expressing tdTomato. *Stem Cells Dev.* **21**, 2981-2986. doi:10.1089/scd.2012.0065

**Kobayashi, H., Sakurai, T., Miura, F., Imai, M., Mochiduki, K., Yanagisawa, E., Sakashita, A., Wakai, T., Suzuki, Y., Ito, T. et al.** (2013). High-resolution DNA methylome analysis of primordial germ cells identifies gender-specific reprogramming in mice. *Genome Res.* **23**, 616-627. doi:10.1101/gr.148023.112

**Kobayashi, T., Zhang, H., Tang, W. W. C., Irie, N., Withey, S., Klisch, D., Sybirna, A., Dietmann, S., Contreras, D. A., Webb, R. et al.** (2017). Principles of early human development and germ cell program from conserved model systems. *Nature* **546**, 416-420. doi:10.1038/nature22812

**Kubota, S. I., Takahashi, K., Nishida, J., Morishita, Y., Ehata, S., Tainaka, K., Miyazono, K. and Ueda, H. R.** (2017). Whole-body profiling of cancer metastasis with single-cell resolution. *Cell Rep.* **20**, 236-250. doi:10.1016/j.celrep.2017.06.010

**Kurimoto, K. and Saitou, M.** (2011). A global single-cell cDNA amplification method for quantitative microarray analysis. *Methods Mol. Biol.* **687**, 91-111. doi:10.1007/978-1-60761-944-4_7

**Kurimoto, K., Yabuta, Y., Ohinata, Y., Ono, Y., Uno, K. D., Yamada, R. G., Ueda, H. R. and Saitou, M.** (2006). An improved single-cell cDNA amplification method for efficient high-density oligonucleotide microarray analysis. *Nucleic Acids Res.* **34**, e42. doi:10.1093/nar/gkl050

**Kurimoto, K., Yabuta, Y., Hayashi, K., Ohta, H., Kiyonari, H., Mitani, T., Moritoki, Y., Kohri, K., Kimura, H., Yamamoto, T. et al.** (2015). Quantitative dynamics of chromatin remodeling during germ cell specification from mouse embryonic stem cells. *Cell Stem Cell* **16**, 517-532. doi:10.1016/j.stem.2015.03.002

**Lawson, K. A., Dunn, N. R., Roelen, B. A. J., Zeinstra, L. M., Davis, A. M., Wright, C. V. E., Korving, J. P. W. F. M. and Hogan, B. L. M.** (1999). Bmp4 is required for the generation of primordial germ cells in the mouse embryo. *Genes Dev.* **13**, 424-436. doi:10.1101/gad.13.4.424

**Leitch, H. G., Blair, K., Mansfield, W., Ayetey, H., Humphreys, P., Nichols, J., Surani, M. A. and Smith, A.** (2010). Embryonic germ cells from mice and rats exhibit properties consistent with a generic pluripotent ground state. *Development* **137**, 2279-2287. doi:10.1242/dev.050427

**Leitch, H. G., McEwen, K. R., Turp, A., Encheva, V., Carroll, T., Grabole, N., Mansfield, W., Nashun, B., Knezovich, J. G., Smith, A. et al.** (2013). Naive pluripotency is associated with global DNA hypomethylation. *Nat. Struct. Mol. Biol.* **20**, 311-316. doi:10.1038/nsmb.2510

**Li, P., Tong, C., Mehrian-Shai, R., Jia, L., Wu, N., Yan, Y., Maxson, R. E., Schulze, E. N., Song, H., Hsieh, C.-L. et al.** (2008). Germline competent embryonic stem cells derived from rat blastocysts. *Cell* **135**, 1299-1310. doi:10.1016/j.cell.2008.12.006

**Magnúsdóttir, E., Dietmann, S., Murakami, K., Günesdogan, U., Tang, F., Bao, S., Diamanti, E., Lao, K., Gottgens, B. and Azim Surani, M.** (2013). A tripartite transcription factor network regulates primordial germ cell specification in mice. *Nat. Cell Biol.* **15**, 905-915. doi:10.1038/ncb2798

**Mallol, A., Guirola, M. and Payer, B.** (2019). PRDM14 controls X-chromosomal and global epigenetic reprogramming of H3K27me3 in migrating mouse primordial germ cells. *Epigenet. Chromatin* **12**, 38. doi:10.1186/s13072-019-0284-7

**McDole, K., Guignard, L., Amat, F., Berger, A., Malandain, G., Royer, L. A., Turaga, S. C., Branson, K. and Keller, P. J.** (2018). In toto imaging and reconstruction of post-implantation mouse development at the single-cell level. *Cell* **175**, 859-876.e833. doi:10.1016/j.cell.2018.09.031

**Nakaki, F., Hayashi, K., Ohta, H., Kurimoto, K., Yabuta, Y. and Saitou, M.** (2013). Induction of mouse germ-cell fate by transcription factors in vitro. *Nature* **501**, 222-226. doi:10.1038/nature12417

**Nakamura, T., Yabuta, Y., Okamoto, I., Aramaki, S., Yokobayashi, S., Kurimoto, K., Sekiguchi, K., Nakagawa, M., Yamamoto, T. and Saitou, M.** (2015). SC3-seq: a method for highly parallel and quantitative measurement of single-cell gene expression. *Nucleic Acids Res.* **43**, e60. doi:10.1093/nar/gkv134

**Northrup, E., Eisenblätter, R., Glage, S., Rudolph, C., Dorsch, M., Schlegelberger, B., Hedrich, H.-J. and Zschemisch, N.-H.** (2011). Loss of Dnd1 facilitates the cultivation of genital ridge-derived rat embryonic germ cells. *Exp. Cell Res.* **317**, 1885-1894. doi:10.1016/j.yexcr.2011.04.013

**Ohinata, Y., Payer, B., O'Carroll, D., Ancelin, K., Ono, Y., Sano, M., Barton, S. C., Obukhanych, T., Nussenzweig, M., Tarakhovsky, A. et al.** (2005). Blimp1 is a critical determinant of the germ cell lineage in mice. *Nature* **436**, 207-213. doi:10.1038/nature03813

**Ohinata, Y., Ohta, H., Shigeta, M., Yamanaka, K., Wakayama, T. and Saitou, M.** (2009). A signaling principle for the specification of the germ cell lineage in mice. *Cell* **137**, 571-584. doi:10.1016/j.cell.2009.03.014

**Okamura, D., Tokitake, Y., Niwa, H. and Matsui, Y.** (2008). Requirement of Oct3/4 function for germ cell specification. *Dev. Biol.* **317**, 576-584. doi:10.1016/j.ydbio.2008.03.002

**Okashita, N., Suwa, Y., Nishimura, O., Sakashita, N., Kadota, M., Nagamatsu, G., Kawaguchi, M., Kashida, H., Nakajima, A., Tachibana, M. et al.** (2016). PRDM14 drives OCT3/4 recruitment via active demethylation in the transition from primed to naive pluripotency. *Stem Cell Rep.* **7**, 1072-1086. doi:10.1016/j.stemcr.2016.10.007

**Rivera-Pérez, J. A., Diefes, H. and Magnuson, T.** (2007). A simple enzymatic method for parietal yolk sac removal in early postimplantation mouse embryos. *Dev. Dyn.* **236**, 489-493. doi:10.1002/dvdy.21034

**Saitou, M. and Yamaji, M.** (2012). Primordial germ cells in mice. *Cold Spring Harb. Perspect. Biol.* **4**, a008375. doi:10.1101/cshperspect.a008375

**Sakashita, A., Kawabata, Y., Jincho, Y., Tajima, S., Kumamoto, S., Kobayashi, H., Matsui, Y. and Kono, T.** (2015). Sex specification and heterogeneity of primordial germ cells in mice. *PLoS ONE* **10**, e0144836. doi:10.1371/journal.pone.0144836

**Shirane, K., Kurimoto, K., Yabuta, Y., Yamaji, M., Satoh, J., Ito, S., Watanabe, A., Hayashi, K., Saitou, M. and Sasaki, H.** (2016). Global landscape and regulatory

principles of DNA methylation reprogramming for germ cell specification by mouse pluripotent stem cells. *Dev. Cell* **39**, 87-103. doi:10.1016/j.devcel.2016.08.008

**Sybirna, A., Tang, W. W. C., Dietmann, S., Gruhn, W. H. and Surani, A. M.** (2019a). A critical but divergent role of PRDM14 in human primordial germ cell fate revealed by inducible degrons. *bioRxiv*.

**Sybirna, A., Wong, F. C. K. and Surani, M. A.** (2019b). Genetic basis for primordial germ cells specification in mouse and human: conserved and divergent roles of PRDM and SOX transcription factors. *Curr. Top. Dev. Biol.* **135**, 35-89. doi:10.1016/bs.ctdb.2019.04.004

**Tang, W. W. C., Kobayashi, T., Irie, N., Dietmann, S. and Surani, M. A.** (2016). Specification and epigenetic programming of the human germ line. *Nat. Rev. Genet.* **17**, 585-600. doi:10.1038/nrg.2016.88

**Weber, S., Eckert, D., Nettersheim, D., Gillis, A. J., Schafer, S., Kuckenberg, P., Ehlermann, J., Werling, U., Biermann, K., Looijenga, L. H. J. et al.** (2010). Critical function of AP-2gamma/TCFAP2C in mouse embryonic germ cell maintenance. *Biol. Reprod.* **82**, 214-223. doi:10.1095/biolreprod.109.078717

**Yabuta, Y., Kurimoto, K., Ohinata, Y., Seki, Y. and Saitou, M.** (2006). Gene expression dynamics during germline specification in mice identified by quantitative single-cell gene expression profiling. *Biol. Reprod.* **75**, 705-716. doi:10.1095/biolreprod.106.053686

**Yamaji, M., Seki, Y., Kurimoto, K., Yabuta, Y., Yuasa, M., Shigeta, M., Yamanaka, K., Ohinata, Y. and Saitou, M.** (2008). Critical function of Prdm14 for the establishment of the germ cell lineage in mice. *Nat. Genet.* **40**, 1016-1022. doi:10.1038/ng.186

**Yamaji, M., Ueda, J., Hayashi, K., Ohta, H., Yabuta, Y., Kurimoto, K., Nakato, R., Yamada, Y., Shirahige, K. and Saitou, M.** (2013). PRDM14 ensures naive pluripotency through dual regulation of signaling and epigenetic pathways in mouse embryonic stem cells. *Cell Stem Cell* **12**, 368-382. doi:10.1016/j.stem.2012.12.012

**Ying, Y. and Zhao, G.-Q.** (2001). Cooperation of endoderm-derived BMP2 and extraembryonic ectoderm-derived BMP4 in primordial germ cell generation in the mouse. *Dev. Biol.* **232**, 484-492. doi:10.1006/dbio.2001.0173